Pyroptosis-Related Genes Regulate Proliferation and Invasion of Pancreatic Cancer and Serve as the Prognostic Signature for Modeling Patient Survival

Wenjing Song
Zhongnan Hospital of Wuhan University
Zhicheng Liu
Zhongnan Hospital of Wuhan University
Kunlei Wang
Zhongnan Hospital of Wuhan University
Kai Tan
Zhongnan Hospital of Wuhan University
Anbang Zhao
Zhongnan Hospital of Wuhan University
Xinyin Li
Zhongnan Hospital of Wuhan University
Yufeng Yuan
Zhongnan Hospital of Wuhan University
Zhiyong Yang (yangzhiyong@whu.edu.cn)
Zhongnan Hospital of Wuhan University

Research Article

Keywords: Pyroptosis, CASP4, Pancreatic ductal adenocarcinoma, Gene signature, Prognosis

Posted Date: March 9th, 2022

DOI: https://doi.org/10.21203/rs.3.rs-1421851/v1

Abstract

Objective: Pancreatic ductal adenocarcinoma (PDAC) has high mortality and poor prognosis. Pyroptosis can influence the prognosis of patients by regulating the proliferation, invasion, and metastasis of cancer cells. However, the role of pyroptosis-related genes (PRGs) in PDAC remains unclear.

Methods: In this study, based on the Cancer Genome Atlas (TCGA) cohort of PDAC samples, univariate Cox analysis and LASSO regression analysis were used to screen the prognostic PRGs and establish the gene signature. To further evaluate the functional significance of CASP4 and NLRP1 in PDAC, we also performed external validation of gene signature using data sets from the GEO database and conducted an in vitro study to examine their effects on PANC-1 cells. The signaling pathway involved in PRGs and its relationship with tumor immunity were also studied. Finally, the regulators upstream of PRGs were predicted by starbase and the relationship between PRGs and anticancer drug sensitivity was analyzed.

Results: A risk prediction model based on CASP4 and NLRP1 was established, which can distinguish high-risk patients from low-risk patients ($P<0.001$). Both internal validation and external GEO data sets validation demonstrate good predictive capability of the model (AUC=0.732, AUC=0.802, AUC=0.632, $P<0.05$). In vitro, CCK8 and Transwell assay suggested that CASP4 may accelerate the progression of PDAC by promoting proliferation and migration of pancreatic cancer cells, while NLRP1 has been found to have tumor suppressive effect. It should be noted that after CASP4 was knocked down, the expression levels of acetyl-CoA carboxylase and SREBP-2 were decreased, and the number of lipid droplets was also significantly reduced. Besides, the expression level of CASP4 was positively correlated with KRAS and P53 mutations. Finally, PRGs were significantly associated with the sensitivity to the inhibitors of AKT and MEK.

Conclusion: PRGs played an important role in tumor immunity and had potential diagnostic, therapeutic and prognostic value for PDAC. In especial, CASP4 can promote tumor progression by promoting the synthesis and accumulation of fatty acids.

Introduction

Pancreatic ductal adenocarcinoma (PDAC) is a kind of digestive system tumor with high malignancy degree and poor prognosis, and 5-year survival rate is less than 10% [1]. With the gradual increase of the incidence, PDAC is projected to become the second leading cause of cancer-related deaths in the United States by 2030 [2, 3]. In China, PDAC had surpassed bladder cancer to become the 7th most common tumor among men, and its mortality rate was also the 7th most common cancer related death in the whole population in 2018 [4]. Today, surgery is still the most radical treatment for PDAC, however, because of the insidious onset, difficulty in early diagnosis and rapid progress of PDAC, most patients have lost best opportunity to operate at the time of diagnosis. Moreover, the resection rate of PDAC is low, and it is not sensitive to conventional radiotherapy and chemotherapy, so the prognosis is usually very poor [5]. The differences in tumor progression and drug susceptibility are closely related to the gene

expression, phenotypic characteristics and cellular component in the tumor microenvironment (TME). Advances in high-throughput sequencing technology and systems biology are contributing to a better understanding of the underlying molecular mechanisms of PDAC and the search for new molecular targets and corresponding therapies to prolong the survival time of patients [6, 7]. In addition, different PDAC subtype classification systems can be established according to the gene characteristics of the tumor at the molecular level, so as to predict the prognosis of patients and select therapeutic drugs [8–11].

Pyroptosis, a kind of programmed cell necrosis that has attracted much attention recently, performed through Gasdermin (GASD) protein family directly [12]. Activated caspase releases the structural domain with the activity of binding membrane phospholipid membrane drilling through cleaving GASD protein, thus inducing pyroptosis [13]. Different from apoptosis which is characterized by immune silencing, pyroptosis shows rupture of cell membrane and the release of many cytokines and danger signaling molecules, which activate the immune system and lead to inflammatory response [14, 15]. Pyroptosis is closely related to various diseases, especially malignant tumors [16], where pyroptosis may play a dual role. On the one hand, pyroptosis can activate the anti-cancer immune response and inhibit the occurrence and progression of cancer. On the other hand, pyroptosis, as a means of pro-inflammatory death, can promote the formation of the TME suitable for tumor cell growth and accelerate cancer growth [17]. Recently, characteristics of pyroptosis-related genes (PRGs) have been shown to be significantly associated with prognosis in ovarian cancer, lung adenocarcinoma, and gastric cancer [18–20]. Therefore, in recent years, researchers have attempted to combine PRGs with various tumor treatments to eliminate malignant cells by regulating pyroptosis [21]. Specifically, A large number of reports have shown that chemotherapy drugs and miRNA can induce the pyroptosis of tumor cells, thus inhibiting the malignant progression of tumor [22–25]. Therefore, it is of great significance to study the relationship between PRGs and prognosis and to explore its expression characteristics and functional involvement in PDAC.

Based on the RNA-seq data and clinicopathological characteristics of TCGA-PAAD dataset, we proposed the signature of PRGs and validated the model by using multiple groups of patient data. In addition, we described the expression of the gene signature at the protein level, and deeply studied the signaling pathway and biochemical process involved in the PRGs and the correlation between PRGs and tumor immunity. Besides, we inferred and studied the other functions of PRGs in pancreatic cancer cells in vitro further. Moreover, we explored the miRNA and transcription factor (TF) regulatory network upstream of PRGs, and analyzed the relationship between PRGs and the drug sensitivity in PDAC, which we hope can contribute to prognostic monitoring and treatment strategies for PDAC patients.

Materials And Methods

Patient data acquisition

We downloaded the RNA-seq, gene mutation data of the pancreatic cancer sample (TCGA-PAAD) and relevant clinical data of the patient (survival time, survival status, age at diagnosis, sex, smoking history, drinking history, diabetes history, history of chronic pancreatitis, tumor site, histological grade, pathological T, N, M, stage, residual tumor and radiotherapy) from the TCGA database (https://portal.gdc.cancer.gov/) on July 10, 2021. RNA-seq data and clinical information from the external validation cohort (ID: GSE62452, GSE57495) were obtained from the Gene Expression Omnibus (GEO) database (https://www.ncbi.nlm.nih.gov/geo/) [26, 27]. After data cleaning, 173 patients in TCGA-PAAD, 64 patients in GSE62452, and 63 patients in GSE57495 had complete survival data.

Gene signature identification and score construction

Based on previous studies and reviews, we extracted 33 PRGs [17, 18, 28–30], as shown in Table. 1. In order to evaluate the prognostic value of PRGs, univariate Cox regression analysis was used to evaluate the correlation between each gene in the TCGA-PAAD cohort and the survival time and survival status of patients. Finally, 11 prognostic PRGs were identified for further analysis. Least absolute shrinkage and selection operator (LASSO) regression analysis was used to identify independent prognostic genes strongly associated with overall survival (OS) in PDAC patients and calculate risk scores. The risk score was calculated by the following formula:

$$\text{Risk score} = \sum_{i=1}^{n} Coef(i) E(i)$$

What needs to be commented is that “n”, “Coef(i)”, E(i) represented the number of signature genes, the coefficient index, and the gene expression level, respectively.

The accuracy and specificity of the model were quantified by the area under the curve (AUC) of receiver operating characteristic (ROC), and then the influence of the included factors on the prognosis of patients was evaluated. The clinicopathological information of the patients and risk score were both included in univariate and multivariate Cox regression analysis, and the risk score based on 2 PRGs was determined to be an independent prognostic factor for PDAC.

Internal and external validation of models

According to the median risk score, patients in TCGA-PAAD and GEO cohort were divided into low-risk group and high-risk group. The survival curve between the risk score and OS of PDAC patients was plotted by Kaplan-Meier (K-M) method, and the difference in survival between the two groups was compared. Similarly, the K-M survival curve between the expression level of PRGs (cutoff at the median expression level) and OS of PDAC patients was plotted, and log-rank was used to test the significance of difference.

Functional inference

Gene Set Enrichment Analysis (GSEA) is a software for gene sets enrichment (https://www.gsea-msigdb.org/gsea/index.jsp) [31, 32]. To clarify differences in gene function and signalling pathways in

different prognosis of PDAC samples, we use GSEA (version 4.0.1) and “enrichplot” R package for enrichment analysis of Gene Ontology (GO) and Kyoto Encyclopedia of Gene and Genomics (KEGG).

Analysis of immune cell infiltration in PDAC

Based on the RNA-seq data, we used the "Cibersort" R package to estimate the abundance of 22 tumor infiltrates immune cells (TIICs) in the single sample [33], and the "ESTIMATE" R package to calculate the matrix and immune scores [34]. The infiltration levels of TIICs and immune scores in different PDAC subclasses were compared and visualize with the box plot. Tumor immune estimate resources (TIMER) (https://cistrome.shinyapps.io/timer/) is a web server for the comprehensive analysis TIICs in TCGA cancer [35–37]. We analyzed the effect of TIICs abundance on the prognosis of patients through “Survival” module and its correlation with PRGs expression by “Correlation” module of TIMER.

Protein expression and survival analysis in HPA

Human protein mapping (HPA) (https://www.proteinatlas.org/) [38–40] provides information on the tissue and cellular distribution of almost all proteins available to the human. In this database, researchers used transcriptomic and proteomic techniques to study protein expression in different human tissues and organs on RNA and protein levels. HPA database was used to analyze the protein expression of PRGs and its relationship with the prognosis of PDAC patients, and the immunohistochemical staining images were also downloaded.

Methylation of CASP4 and landscape analysis of gene mutation

The human disease methylation database, DiseaseMeth version 2.0 is a an interactive database focused on the aberrant DNA methylation in human diseases, especially various cancers. We used this website to analyze and compare the differences in CASP4 methylation between PDAC and para-cancer tissues and visualized them with box diagrams. R packet “maftools” was used to compare the frequency of individual gene mutations in TCGA-PAAD.

Potential regulation of PRGs

We used TRRUST (version 2) (https://www.grnpedia.org/trrust/) [41], an expanded reference database of human and mouse transcriptional regulatory interactions for TF-PRGs interaction analysis. The upstream miRNA that can inhibit the expression of PRGs in PDAC were predicted by Starbase (http://starbase.sysu.edu.cn/), and the corresponding correlation curves of miRNA-mRNA were plotted at the same time.

Analysis of drug sensitivity related to PRGs

GSCALite (http://bioinfo.life.hust.edu.cn/web/GSCALite/) [42] is a comprehensive cancer analysis database that combines gene expression analysis, immunoinvasion analysis, mutation analysis and drug sensitivity analysis, containing 33 types of cancer from TCGA and GDSC. Through the "Drug Sensitivity

Analysis" module of Genomics of Drug Sensitivity in Cancer (GDSC), we studied the correlation between PRGs and drug resistance in PDAC.

Cell culture and transfection

Human pancreatic cancer cell line PANC-1, purchased from China Center for Type Culture Collection (CCTCC), was cultured with special medium (CM-0627, Procell Life Science & Technology Co., Ltd.) in the 37°C cell incubator containing 5% CO_2. Following the manufacturer's instructions, siRNA (siCASP4: 5'-GGGUCUGGACUAUAGUGUATT-3' and 5'-UACACUAUAGUCCAGACCCTT-3, siNLRP1：5'-CGGUGACCGUUGAGAUUGATT-3' and 5'-UCAAUCUCAACGGUCACCGTT-3') were transfected into cells.

Real-time PCR

Following the manufacturer's instructions, total RNA was extracted from cells with Trizol reagent (Invitrogen, Carlsbad, CA) and then measured using a NanoDrop ND-2000 spectrophotometer (Thermo Fisher Scientific). The RNA was reverse transcribed into cDNA using HiScript II Q RT SuperMix for qPCR (+ gDNA Wiper) (R223-01, Vazyme, China). ChamQ Universal SYBR qPCR Master Mix (Q711-02, Vazyme, China) was used for qPCR. QPCR primers include CASP4, NLRP1, FASN, ACC, SREBP-1 and SREBP-2. The primer sequences used are listed in Table S1. Gene expression was normalized to the expression of GAPDH and calculated using $2^{-\Delta\Delta CT}$ method. Three repeated experiments were set up in each group.

Western blotting

48h after siRNA transfection, the cells were washed twice with PBS. RIPA Lysis Buffer (BL504A, Biosharp, China) supplemented with protease and phosphatase inhibitors was added to the cells and lysed on ice for 15 minutes. The liquid was collected and centrifuged. Protein concentration was determined using BCA protein determination kit (P0012, Beyotime, China). Total protein was transferred to PVDF membrane (Millipore, Billerica, MA) after electrophoresis in 10% or 7.5% SDS-PAGE. After blocking the nonspecific sites on the membrane with 5% sealant for 1h at room temperature, the membrane was applied to CASP4 (1:1000, #4450, Cell Signaling Technology, USA), NLRP1(1: 1000, ab36852, abcam, USA), GAPDH (1:5000, 10494-1-AP, Proteintech) and incubated overnight at 4°C. Then, the membrane was incubated with HRP-Conjugated Affinipure Goat Anti-Rabbit IgG(H + L) (SA00001-2, Proteintech) at room temperature for 1h. The blots were finally visualized with the ECL Chemiluminescence substrate (hypersensitive) (BL523B, Biosharp, China) and ECL reagents (Tanon, Shanghai, China) and quantified using Image J (1.46R). Three repeated experiments were set up in each group.

Cell proliferation assay

24h after siRNA transfection, the cells were transfected into a 96-well culture plate (2000 cells/well). Following the manufacturer's instructions, add 100μL/well diluted 10 times CCK-8 reagent (CA1210, Beijing Solarbio Science & Technology Co., Ltd.) at 0, 24, 48, 72h after laying plate, respectively. The cells were incubated at 37°C for 2 hours and the optical density (OD) at 450 nm was measured with a microplate reader. Three repeated experiments were set up in each group.

Transwell invasion assay

Transparent PET Membrane 24 Well 8.0 μm tin (BD Biosciences, USA) was used for cell invasion ability detection. 24h after siRNA transfection, 2×10^4 cells were inoculated into the upper chamber, and 500ul of complete medium was added into the lower chamber. After the cell morphology was restored, the cells were starved for 8h. Then the medium containing 20%FBS was changed into the lower chamber to induce membrane penetration. 24h later, it was fixed with 4% paraformaldehyde for 30 minutes and stained with crystal violet for 15 minutes. Images were taken under microscope and analyzed by Image J (1.46R). Three repeated experiments were set up in each group.

BODIPY staining

BODIPY staining was used to observe the neutral lipid droplets in PANC-1 cells after treatment. Panc-1 cells were inoculated on cover glass, and when the cell density reached 50%-70%, they were cleaned with PBS for 3 times. The cells were fixed with 4% paraformaldehyde for 15min and then cleaned with PBS again. Then, 2uM BODIPY 493/503 (D3922, Thermo Scientific) was used to avoid light Staining for 30min, and DAPI Staining Solution (C1005, Beyotime) was used to avoid light Staining for 5min. After staining, soak with PBS for 3 times. Place the cover slide lightly on the slide dripping with antifade mounting medium (P0126, Beyotime) and observe under a fluorescence microscope (Olympus, BX53).

Statistical analysis

The research flow chart has been shown in Fig. 1. All survival curves are displayed with p-value from log-rank test. Mean and median for continuous variables were compared using independent t-test when the data were normally distributed; otherwise, the Mann-Whitney U test was used. Comparison of clinicopathological parameters and other classified variables was tested by chi-square test. The correlation of gene expression was evaluated by Spearman's correlation and statistical significance. All tests were two-sided and P-value < 0.05 were considered statistically significant. The box plots were drawn online with imageGP (http://www.ehbio.com/ImageGP/index.php/Home/Index/index.html).

Results

Gene signature identification and risk scoring model construction

The selected PRGs (Table. 1) were used for GO and KEGG analysis, and the results showed that these genes regulated multiple IL-1β related pathways (Figure. 2). Firstly, a univariate Cox regression analysis was used to identify 11 PRGs associated with OS in TCGA-PAAD patients (P < 0.05) (Table 2). To identify the most powerful prognostic gene markers, LASSO regression analysis was used to screen two PRGs and construct a prognostic gene signature (Fig. 3A), thus minimizing the risk of overfitting. The risk score of patients was calculated based on the expression level and regression coefficient, which was as follows: Risk score = -0.0072015395171821 4* (the expression of NLRP1) + 0.0344857322413964* (the expression of CASP4). PDAC patients were divided into low-risk group (n = 87) and high-risk group (n = 86) according to the median risk score. To further evaluate the impact of risk score on the prognosis of

PDAC patients, K-M analysis showed that the prognosis of high-risk group was significantly poorer than that of low-risk group ($P < 0.001$) (Fig. 3B). The distribution of survival status and risk scores of patients was shown in Fig. 3C-3D, indicating that by the time of follow-up, more PDAC patients had died in the high-risk group than in the low-risk group. The ROC curve showed good predictive power of the model for predicting the prognosis of PDAC patients based on the gene signature (AUC = 0.732, $P < 0.001$) (Fig. 3E).

Table 1
33 pyroptosis-related genes.

Gene	Full-name
AIM2	Absent in melanoma 2
CASP1	cysteine-aspartic acid protease-1
CASP3	cysteine-aspartic acid protease-3
CASP4	cysteine-aspartic acid protease-4
CASP5	cysteine-aspartic acid protease-5
CASP6	cysteine-aspartic acid protease-6
CASP8	cysteine-aspartic acid protease-8
CASP9	cysteine-aspartic acid protease-9
ELANE	elastase, neutrophil expressed
GPX4	glutathione peroxidase 4
GSDMA	gasdermin A
GSDMB	gasdermin B
GSDMC	gasdermin C
GSDMD	gasdermin D
GSDME	gasdermin E
IL18	interleukin 18
IL1B	interleukin 1 beta
IL6	interleukin 6
NLRC4	NLR family CARD domain containing 4
NLRP1	NLR family pyrin domain containing 1
NLRP2	NLR family pyrin domain containing 2
NLRP3	NLR family pyrin domain containing 3
NLRP6	NLR family pyrin domain containing 6
NLRP7	NLR family pyrin domain containing 7
NOD1	nucleotide binding oligomerization domain containing 1
NOD2	nucleotide binding oligomerization domain containing 2
PJVK	pejvakin/deafness, autosomal recessive 59

Gene	Full-name
PLCG1	phospholipase C gamma 1
PRKACA	protein kinase cAMP-activated catalytic subunit alpha
PYCARD	PYD and CARD domain containing
SCAF11	SR-related CTD associated factor 11
TIRAP	TIR domain containing adaptor protein
TNF	tumor necrosis factor

Table 2
Tree diagram of univariate Cox regression between PRGs and prognosis of PDAC.

ID	HR	HR.95L	HR.95H	pvalue
NLRP2	1.080016	1.022584	1.140673	0.005762
CASP8	1.269678	1.09664	1.470019	0.001403
PRKACA	0.89609	0.83489	0.961776	0.002368
NLRP1	0.873237	0.784275	0.97229	0.013415
PYCARD	1.023932	1.004007	1.044253	0.018333
PLCG1	0.87138	0.778094	0.975849	0.017166
CASP1	1.081328	1.006057	1.16223	0.033669
GSDMC	1.103778	1.011484	1.204493	0.026673
IL18	1.050832	1.023062	1.079355	0.000285
AIM2	1.105527	1.020615	1.197503	0.013878
CASP4	1.204421	1.110487	1.306301	7.14E-06

In order to further analyse the prognostic value of PRGs characteristics in PDAC patients, univariate and multivariate Cox regression analyses were performed on clinicopathological characteristics, including age at diagnosis, sex, smoking history, drinking history, diabetes history, history of chronic pancreatitis, tumor site, histological grade, pathological T, N, M, stage, residual tumor and radiotherapy, and risk score. The results indicated that risk score based on PRGs signature was a independent prognostic factor for PDAC patients (P = 0.001, HR = 3.650, 95%CI:1.473–6.304) (Fig. 3F-3G).

External validation of the gene signature

In order to further verify the effect value of the gene signature based on PRGs, we downloaded two datasets, GSE57495 and GSE62452, from GEO. After removing the samples with 0 gene expression and

the samples that without survival information, a total of 63 and 64 samples were included for external verification respectively. The risk score of the sample of data set was calculated according to the formula, and the patients were also divided into low-risk group and high-risk group. K-M analysis showed that the prognosis of the high-risk group was significantly worse than that of the low-risk group (P = 0.008, P = 0.002) (Fig. 4A&5A). More PDAC patients in the high-risk group had died by the time of follow-up and had survived less than those in the low-risk group (Fig. 4C-4D&5C-5D). The ROC curve showed that the model had good predictive ability (AUC = 0.802, AUC = 0.632, P < 0.05) (Fig. 4B&5B).

Function inference and potential regulation of PRGs

GSEA analysis displayed that the DEGs highly expressed in the high-risk group were mainly involved in the regulation of antigen processing and presentation, regulation of DNA transcription and NF-κB signaling pathway. In addition, it was also related to proteasome, post-transcriptional splicing of DNA, nucleotide excision repair and p53 signal pathways (Figure S1A). Based on the association between pyroptosis and tumor immunity, we evaluated the infiltration of TIICs in PDAC samples and found that there were more infiltration of macrophage M1 and Tfh in the high-risk group (P < 0.05) (Figure S1B). Furthermore, we analyzed the influence of infiltration abundance of macrophage M1 and Tfh on the prognosis of PDAC patients and its correlation with the expression levels of NLRP1 and CASP4 by TIMER website. The results showed that high infiltration of macrophage M1 was associated with poorer prognosis (HR = 1.29, P = 0.013), while infiltration abundance of Tfh was not associated significantly with prognosis (HR = 0.885, P = 0.237) (Figure S1C). NLRP1 was correlated positively with the infiltration of macrophage M1 and Tfh (r = 0.29, P < 0.001; r = 0.281, P < 0.001) (Figure S1D). CASP4 showed a significant positive correlation with the infiltration of macrophage M1 (r = 0.457, P < 0.001), but no significant correlation with the infiltration of Tfh (r = 0.102, P = 0.184) (Figure S1E).

The starbase online prediction website was used to predict the upstream regulatory miRNA of NLRP1 and CASP4, and three miRNA that could regulate PRGs in PDAC were screened (Figure S2A&E). Among them, the potential regulatory miRNA upstream of NLRP1 include miR-30a-5p (r=-0.162, P = 0.030), miR-181b-5p (r=-0.210, P = 0.005) and miR-143-3p (r=-0.168, P = 0.025) (Figure S2B-9D). miR-381-3p (r=-0.313, P < 0.001), miR-382-5p (r=-0.253, P < 0.001) and miR-409-3p (r=-0.340, P < 0.001) may inhibit the expression of CASP4 in PDAC (Figure S2F-H). Figure S2I depicted the networks of the top 25 TF with a strong regulatory relationship between NLRP1 and CASP4.

Expression and survival analysis of PRGs

Moreover, we compared the expression of PRGs in cancer and adjacent tissues and found that the mRNA levels of CASP4 in PDAC tissue were higher than those in normal pancreatic tissue (P < 0.05) (Fig. 6A). To further analyse the reasons for the difference in CASP4 expression between cancer and para-cancer, we used DiseaseMeth database to compare the methylation level of CASP4. The results showed that CASP4 was located at two sites on the chromosome in which the mean methylation level of CASP4 in PDAC was significantly lower than in para-cancer tissues (P < 0.05) (Fig. 6B).

Besides, the survival curve showed that high expression of NLRP1 and low expression of CASP4 at both mRNA and protein levels were associated with a better prognosis ($P < 0.05$) (Fig. 6D-G), and there was a significant negative correlation between NLRP1 expression and CASP4 expression in PDAC ($r=-0.42$, $P < 0.001$) (Fig. 6C). Figure. 6H, exhibiting the immunohistochemical staining and intensity of NLRP1 and CASP4 proteins in all PDAC samples, showed that NLRP1 staining was weak, while the protein expression level of CASP4 were elevated in PDAC samples (Fig. 6I-J).

PRGs regulate the proliferation and invasion of pancreatic cancer cells in vitro

To further evaluate the functional significance of CASP4 and NLRP1 in PDAC, we conducted an in vitro study to examine the effects of CASP4 and NLRP1 on PANC-1. First, RNA and protein expression levels of CASP4 and NLRP1 in PANC-1 cells were knocked down by transfection of siRNA ($P < 0.01$) (Fig. 7A-7B). CCK-8 showed that CASP4 knockdown significantly inhibited the cell viability of PANC-1, while NLRP1 knockdown significantly enhanced the cell viability ($P < 0.01$) (Fig. 7C). In addition, Transwell results ($P < 0.01$) showed that knocking down CASP4 significantly inhibited the invasion and migration of PANC-1, which were promoted by knocking down NLRP1 (Fig. 7D). These results suggested that CASP4 may accelerate the progression of PDAC by promoting proliferation, invasion and migration of pancreatic cancer cells, while NLRP1 has been found to have tumor suppressive effect in vitro.

CASP4 was associated with KRAS and P53 mutations potentially as well as could regulate accumulation of lipid droplets

It is well known that CASP4, as a PRG, can promote pyroptosis. However, according to data analysis and in vitro experimental results, CASP4 has been proved to be an oncogene, which can promote tumor invasion and migration. Therefore, we inferred that CASP4 may have other biological functions to play the role of promoting cancer. KRAS and P53 mutations are most common in pancreatic cancer (Fig. 8A-B). Based on this, PDAC samples were grouped according to KRAS and P53 mutations, and we compared the expression level of CASP4 in mutant and wild-type tumors. We found that the expression level of CASP4 was higher in both KRAS mutated samples and P53 mutated samples than in wild-type samples ($P < 0.001$) (Fig. 8C). Meanwhile, correlation analysis also showed that CASP4 was significantly positively correlated with KRAS and P53 expression level respectively ($R = 0.45$, $R = 0.19$, $P < 0.001$) (Fig. 8D). In addition, gene sets enrichment analysis also suggested that the differential genes in CASP4 high expression samples were mainly involved in regulating programmed cell death, nucleotide metabolism and P53 signaling pathway (Fig. 8E).

To further explore the mechanism of CASP4 promoting cancer, we knocked down CASP4 by transfection with shRNA in PANC-1 cells, and then detected the expression of key enzyme molecules in fatty acid synthesis. The results showed that low CASP4 expression significantly reduced the RNA levels of acetyl-CoA carboxylase (ACC) ($P < 0.001$) and SREBP-2 ($P < 0.05$) (Fig. 9A). In addition, we used BODIPY 493/503 fluorescent dye to visually observe the number of lipid droplets in PANC-1 cell (Fig. 9B-9C) and

found that the number of lipid droplets decreased significantly after CASP4 knockdown (40 vs. 22, $P < 0.05$).

Analysis of drug sensitivity of PRGs

Figure 10, displaying the correlation analysis between PRGs and drug sensitivity in PDAC, showed that CASP4 was significantly positively related with FK866, the inhibitor of nicotinamide phosphoribosyltransferase and vorinostat, the inhibitor of histone deacetylase inhibitors of sensitivity, and NLRP1 negatively correlated with them. In addition, CASP4 was negatively correlated with 17-AAG, the inhibitor of AKT, Mirdametinib (PD-0325901), Refametinib(RDEA-119), CI-1040, and Trametinib, the inhibitors of MEK.

Discussion

PDAC is one of the most malignant digestive tract tumors, whose mortality and morbidity are almost the same and the 5-year overall survival rate is only about 9% [43]. At present, surgical treatment is still the radical treatment for PDAC. However, due to the hidden onset of pancreatic cancer, most of PDAC cannot be removed by surgery at the time of discovery. The lack of effective tumor biomarkers to evaluate the prognosis of PDAC and the difficulty in developing personalized treatment plan have resulted in a low survival rate [44, 45]. Tumorigenesis is associated with a variety of factors, including activation of proto-oncogenes and anticancer genes, TME, oxidative stress, and chronic inflammatory stimuli. Activation of pyroptosis leads to the release of the inflammatory mediators IL-1 and IL-18, which can contribute to the development of cancer in a number of ways. For another, pyroptosis can promote tumor cell death, making it a potential prognostic marker and therapeutic target for cancer. Therefore, PRGs play different roles in the occurrence and progression of different cancers. For example, pyroptosis inhibits the progression of hepatocellular carcinoma, colorectal cancer and gastric cancer [46–51], but it promotes the proliferation and metastasis of breast cancer cells [52]. However, the role of PRGs in PDAC has not been clarified. Therefore, in this study, we aimed to discover a novel prognostic marker related to pyroptosis through data analysis and mechanism exploration to provide potential approaches in the treatment of PDAC.

Firstly, we obtained the mRNA expression levels of 33 currently known PRGs in TCGA-PAAD samples. In order to further evaluate the prognostic value of these PRGs, we constructed a risk score model based on NLRP1 and CASP4 gene signature through univariate Cox analysis and LASSO regression analysis, and then verified their good predictive performance in external datasets. Patients in the high-risk group fared worse when grouped by risk score, and the same conclusion was obtained from external data, further demonstrating the specificity and accuracy of this PRGs signature in distinguishing different prognostic PDAC. Based on epidemiological studies, previous cohort studies and expert consensus [53–60],We included a variety of clinical pathological factors that may affect OS in PDAC patients and the result showed that risk score was found to be an independent prognostic factor, further proving the great influence of PRGs on the prognosis of PDAC. However, the above factors have no obvious effect on the

OS of PDAC, which may be due to the lack of patient data, as only 43 patients were included with complete data.

Previous studies have shown that NLRP1 is considered a tumor suppressor gene. NLRP1 is one of inflammasome sensors, the activator of which induces the proteasome-mediated destruction of the N-terminal fragment and liberates the C-terminal fragment to form an inflammasome [61]. Inflammasome represents a group of protein complexes that induce inflammation and pyroptosis, and its abnormal and chronic activation is the pathological basis for many common inflammatory diseases and tumorigenesis [62]. Studies have indicated that NLRP1 mediates the production of IL-18 to help prevent colorectal cancer associated with colitis [49]. Targeting the activation of NLRP1 in epidermal keratinocytes represented a potential therapeutic strategy for NLRP1-dependent inflammatory skin disease and cancer [63, 64]. The prognostic significance of CASP4 overexpression in cancers remains controversial. For example, the clinical cohort study of Shibamoto et al. showed that CASP4 may play a role as a tumor suppressor gene in esophageal cancer and as a potential biomarker for predicting esophageal cancer prognosis [65, 66]. However, silencing CASP4 gene inhibited the migration, adhesion, and invasion of epithelial cancer cells [67]. Terlizzi et al. reached a similar conclusion in non-small cell lung cancer (NSCLC), which means that CASP4 overexpression was associated with poor prognosis in NSCLC patients [68]. Meng et al. found that CASP4 was highly expressed in renal clear cell carcinoma based on TCGA data, suggesting poor prognosis, and was associated with tumor drug resistance [69]. In our study, high expression of CASP4 may be associated with poor prognosis in PDAC patients, while NLRP1 is thought to play a tumor suppressor role, and similar expression differences were found on protein levels. Moreover, CCK8 and transwell assay suggested that CASP4 may accelerate the progression of PDAC by promoting proliferation and migration of pancreatic cancer cells, while NLRP1 has been found to have tumor suppressive effect in vitro. It is noteworthy that CASP4 is commonly known as a cell pyroptosis gene, but it has been found to promote cancer in some experimental and clinical studies, the mechanism of which has not been explored. In order to explore the potential mechanism of CASP4 regulating tumor progression, we compared DEGs in the high and low CASP4 expression groups and found that in addition to significant differences in programmed cell death, more DEGs were enriched in P53 signaling pathway and nucleotide metabolism pathway. In addition, Michela Terlizzi analyzed changes in lipid metabolism characteristics in CASP4-positive NSCLC and found increased palmitic acid and malonic acid in tissues of CASP4-positive patients, which are important for fatty acid biosynthesis and elongation [70, 71]. KRAS and P53 mutations, the most common mutation in pancreatic cancer, can change normal metabolic pathways and initiate metabolic reprogramming by activating transcription factors and enhancing enzyme activity [72]. Moreover, recent studies have found that KRAS and P53 play a synergistic role mediated by transcription factors in promoting pancreatic cancer metastasis [73]. By grouping pancreatic cancer samples in TCGA, we found that the expression level of CASP4 was higher in both KRAS mutation samples and P53 samples than in wild-type samples. Therefore, it is reasonable to speculate that CASP4 may be one of the factors in the synergistic regulatory network of KRAS and P53 and promoted the biosynthesis of fatty acids in pancreatic cancer and reserves productive substrates for the proliferation and migration of tumor cells in addition to the occurrence of pyroptosis. Our experiment results

suggested that CASP4 knockdown in PANC-1 cells significantly reduces the number of lipid droplets, and the expression of key enzymes and transcription factors involved in fatty acid synthesis (ACC and SREBF-2), which was the first in vitro study of CASP4 regulation of pancreatic cancer lipid metabolism. This will pave the way for further exploration of CASP4 gene function in the future.

Functional analysis showed that the DEGs between the low-risk and high-risk groups were closely related to antigen presentation, gene transcription, cleavage of pyroptosis-related proteins and some classical cancer pathways. Due to the fact that pyroptosis is usually associated with the release of pro-inflammatory factors and activation of the immune system, we compared the abundance of TIICs in the high and low risk groups and found that there were more macrophage M1 and Tfh in the high-risk group. Survival analysis also showed that infiltration of macrophage M1 predicted poor prognosis. Macrophages are the most abundant cells in tumor stroma and have strong plasticity and play a variety of functions in the TME. Among them, macrophage M1 have the ability to kill tumor cells, while the other part, tumor-related macrophages, usually manifested as macrophage M2, show anti-inflammatory and tumor-promoting effects [74]. Tfh plays an important role in promoting differentiation of B cell and inducing antibody responses in humoral immunity and immune-related inflammatory diseases, including infection, autoimmune diseases and cancer. Tfh induces the formation of ectopic lymphoid structures at tumor sites and recruits CD8 + T cells, macrophages and natural killer (NK) cells involved in anti-tumor immunity to suppress tumor growth [75]. Wu et al. also found higher levels of Tfh infiltration in the high-risk group when predicting prognosis in PDAC patients [76]. The analysis of the infiltration of TIICs further explained the mechanism of the effect for pyroptosis on the occurrence and development of cancer, and provided a glimmer of hope for the immunotherapy of PDAC.

We tried to apply the results of this study into clinical practice, not only establishing a prognostic risk model, but also exploring the correlation between PRGs and tumor drug resistance. Through drug sensitivity analysis, CASP4 was significantly related with the inhibitors of AKT and MEK. This further suggested that CASP4 may be involved in tumor cell lipid metabolism through AKT and MAPK signaling pathways, which also provided evidence for the regulatory relationship between CASP4 and KRAS mutation. Our research focuses on predicting the diagnostic, therapeutic and prognostic value of PRGs in PDAC from the perspective of bioinformatics and in vitro experiments, and exploring the regulation of CASP4 on lipid metabolism in pancreatic cancer for the first time in vitro. However, we have to say that this study is a retrospective study with some limitations. Therefore, we call for a prospective study with a larger sample size to verify the clinical application of PRGs in personalized management of PDAC patients. Besides, this study concluded that there was a lack of a series of in-depth experimental verification, such as the regulatory mechanism between CASP4 and KRAS/MEK signaling pathway and genes specifically regulated by CASP4 in regulating lipid metabolism. As a continuation of future research, we will supplement it in future research.

Conclusions

In this study, we used TCGA-PAAD RNA-seq data and clinical data to construct a risk prediction model based on PRGs. The risk score calculated based on the expression level of NLRP1 and CASP4 is an independent prognostic factor for PDAC patients. In addition to pyroptosis, CASP4 may promote pancreatic cancer cell migration by promoting fatty acid synthesis. PRGs, especially CASP4 are expected to be important prognostic markers and therapeutic targets for PDAC, and corresponding targeted drugs are emerging.

Abbreviations

PDAC	Pancreatic ductal adenocarcinoma
PRGs	Pyroptosis-related genes
TCGA	The Cancer Genome Atlas
Tfh	T cells follicular helper
TF	Transcription factor
TME	Tumor microenvironment
GASD	Gasdermin
GEO	Gene Expression Omnibus
CDF	Cumulative distribution function
LASSO	Least absolute shrinkage and selection operator
AUC	Area under the curve
ROC	Receiver operating characteristic
K-M	Kaplan-Meier
GSEA	Gene Set Enrichment Analysis
GO	Gene Ontology
KEGG	Kyoto Encyclopedia of Gene and Genomics
TIICs	Tumor infiltrates immune cells
TIMER	Tumor immune estimate resources
HPA	Human protein mapping
GDSC	Genomics of Drug Sensitivity in Cancer
CCTCC	China Center for Type Culture Collection
DEGs	Differentially expressed genes
Tregs	T cells regulatory
NSCLC	non-small cell lung cancer
NK	natural killer

Declarations

Acknowledgments

The authors thank the contributors of the TCGA and GEO databases.

Funding

This work was supported by Cancer research and translational platform project of Zhongnan Hospital of Wuhan University (ZLYNXM202004).

Authors' contributions

All authors contributed to the article and approved the submitted version. Wenjing Song and Zhicheng Liu contributed to the conception and design of the study. Kunlei Wang and Anbang Zhao were involved with data interpretation. Xinyin Li and Kai Tan helped with the revision of manuscript and submit proposal. Zhiyong Yang and Yufeng Yuan were involved with revision of the article for important intellectual content, reading and approving the final version of the submitted manuscript as well as coordinating the entire process.

Ethics approval and consent to participate

Not applicable.

Consent for publication

Not applicable.

Competing interest

The authors declare that they have no conflicts of interest.

Availability of data and materials

The datasets generated and/or analysed during the current study are available in the TCGA (https://portal.gdc.cancer.gov/) and GEO (https://www.ncbi.nlm.nih.gov/geo/) (GSE62452; GSE57495). The data that support the findings of this study are available from the corresponding author upon reasonable request.

References

1. Kleeff J, Korc M, Apte M, La Vecchia C, Johnson CD, Biankin AV, Neale RE, Tempero M, Tuveson DA, Hruban RH *et al*: **Pancreatic cancer**. *Nat Rev Dis Primers* 2016, **2**:16022.
2. Balachandran VP, Beatty GL, Dougan SK: **Broadening the Impact of Immunotherapy to Pancreatic Cancer: Challenges and Opportunities**. *Gastroenterology* 2019, **156**(7):2056-2072.
3. Rahib L, Smith BD, Aizenberg R, Rosenzweig AB, Fleshman JM, Matrisian LM: **Projecting cancer incidence and deaths to 2030: the unexpected burden of thyroid, liver, and pancreas cancers in the United States**. *Cancer Res* 2014, **74**(11):2913-2921.

4. Sun D, Cao M, Li H, He S, Chen W: **Cancer burden and trends in China: A review and comparison with Japan and South Korea**. *Chin J Cancer Res* 2020, **32**(2):129-139.
5. Bray F, Ferlay J, Soerjomataram I, Siegel RL, Torre LA, Jemal A: **Global cancer statistics 2018: GLOBOCAN estimates of incidence and mortality worldwide for 36 cancers in 185 countries**. *CA Cancer J Clin* 2018, **68**(6):394-424.
6. Neoptolemos JP, Kleeff J, Michl P, Costello E, Greenhalf W, Palmer DH: **Therapeutic developments in pancreatic cancer: current and future perspectives**. *Nat Rev Gastroenterol Hepatol* 2018, **15**(6):333-348.
7. McGuigan A, Kelly P, Turkington RC, Jones C, Coleman HG, McCain RS: **Pancreatic cancer: A review of clinical diagnosis, epidemiology, treatment and outcomes**. *World J Gastroenterol* 2018, **24**(43):4846-4861.
8. Feng Z, Shi M, Li K, Ma Y, Jiang L, Chen H, Peng C: **Development and validation of a cancer stem cell-related signature for prognostic prediction in pancreatic ductal adenocarcinoma**. *J Transl Med* 2020, **18**(1):360.
9. Yue P, Zhu C, Gao Y, Li Y, Wang Q, Zhang K, Gao S, Shi Y, Wu Y, Wang B *et al*: **Development of an autophagy-related signature in pancreatic adenocarcinoma**. *Biomed Pharmacother* 2020, **126**:110080.
10. Xu D, Wang Y, Zhou K, Wu J, Zhang Z, Zhang J, Yu Z, Liu L, Liu X, Li B *et al*: **Identification of an extracellular vesicle-related gene signature in the prediction of pancreatic cancer clinical prognosis**. *Biosci Rep* 2020, **40**(12).
11. Xu F, Zhang Z, Zhao Y, Zhou Y, Pei H, Bai L: **Bioinformatic mining and validation of the effects of ferroptosis regulators on the prognosis and progression of pancreatic adenocarcinoma**. *Gene* 2021, **795**:145804.
12. Shi J, Gao W, Shao F: **Pyroptosis: Gasdermin-Mediated Programmed Necrotic Cell Death**. *Trends Biochem Sci* 2017, **42**(4):245-254.
13. Broz P, Pelegrín P, Shao F: **The gasdermins, a protein family executing cell death and inflammation**. *Nat Rev Immunol* 2020, **20**(3):143-157.
14. Frank D, Vince JE: **Pyroptosis versus necroptosis: similarities, differences, and crosstalk**. *Cell Death Differ* 2019, **26**(1):99-114.
15. Wang Q, Wang Y, Ding J, Wang C, Zhou X, Gao W, Huang H, Shao F, Liu Z: **A bioorthogonal system reveals antitumour immune function of pyroptosis**. *Nature* 2020, **579**(7799):421-426.
16. Fang Y, Tian S, Pan Y, Li W, Wang Q, Tang Y, Yu T, Wu X, Shi Y, Ma P *et al*: **Pyroptosis: A new frontier in cancer**. *Biomed Pharmacother* 2020, **121**:109595.
17. Xia X, Wang X, Cheng Z, Qin W, Lei L, Jiang J, Hu J: **The role of pyroptosis in cancer: pro-cancer or pro-"host"?** *Cell Death Dis* 2019, **10**(9):650.
18. Ye Y, Dai Q, Qi H: **A novel defined pyroptosis-related gene signature for predicting the prognosis of ovarian cancer**. *Cell Death Discov* 2021, **7**(1):71.

19. Lin W, Chen Y, Wu B, Chen Y, Li Z: **Identification of the pyroptosis-related prognostic gene signature and the associated regulation axis in lung adenocarcinoma**. *Cell Death Discov* 2021, **7**(1):161.
20. Shao W, Yang Z, Fu Y, Zheng L, Liu F, Chai L, Jia J: **The Pyroptosis-Related Signature Predicts Prognosis and Indicates Immune Microenvironment Infiltration in Gastric Cancer**. *Front Cell Dev Biol* 2021, **9**:676485.
21. Fulda S: **Targeting apoptosis for anticancer therapy**. *Semin Cancer Biol* 2015, **31**:84-88.
22. Yue E, Tuguzbaeva G, Chen X, Qin Y, Li A, Sun X, Dong C, Liu Y, Yu Y, Zahra SM *et al*: **Anthocyanin is involved in the activation of pyroptosis in oral squamous cell carcinoma**. *Phytomedicine* 2019, **56**:286-294.
23. Chen L, Weng B, Li H, Wang H, Li Q, Wei X, Deng H, Wang S, Jiang C, Lin R *et al*: **A thiopyran derivative with low murine toxicity with therapeutic potential on lung cancer acting through a NF-κB mediated apoptosis-to-pyroptosis switch**. *Apoptosis* 2019, **24**(1-2):74-82.
24. Pizato N, Luzete BC, Kiffer L, Corrêa LH, de Oliveira Santos I, Assumpção JAF, Ito MK, Magalhães KG: **Omega-3 docosahexaenoic acid induces pyroptosis cell death in triple-negative breast cancer cells**. *Sci Rep* 2018, **8**(1):1952.
25. Wang L, Li K, Lin X, Yao Z, Wang S, Xiong X, Ning Z, Wang J, Xu X, Jiang Y *et al*: **Metformin induces human esophageal carcinoma cell pyroptosis by targeting the miR-497/PELP1 axis**. *Cancer Lett* 2019, **450**:22-31.
26. Yang S, He P, Wang J, Schetter A, Tang W, Funamizu N, Yanaga K, Uwagawa T, Satoskar AR, Gaedcke J *et al*: **A Novel MIF Signaling Pathway Drives the Malignant Character of Pancreatic Cancer by Targeting NR3C2**. *Cancer Res* 2016, **76**(13):3838-3850.
27. Chen DT, Davis-Yadley AH, Huang PY, Husain K, Centeno BA, Permuth-Wey J, Pimiento JM, Malafa M: **Prognostic Fifteen-Gene Signature for Early Stage Pancreatic Ductal Adenocarcinoma**. *PLoS One* 2015, **10**(8):e0133562.
28. Karki R, Kanneganti TD: **Diverging inflammasome signals in tumorigenesis and potential targeting**. *Nat Rev Cancer* 2019, **19**(4):197-214.
29. Wang B, Yin Q: **AIM2 inflammasome activation and regulation: A structural perspective**. *J Struct Biol* 2017, **200**(3):279-282.
30. Man SM, Kanneganti TD: **Regulation of inflammasome activation**. *Immunol Rev* 2015, **265**(1):6-21.
31. Subramanian A, Tamayo P, Mootha VK, Mukherjee S, Ebert BL, Gillette MA, Paulovich A, Pomeroy SL, Golub TR, Lander ES *et al*: **Gene set enrichment analysis: a knowledge-based approach for interpreting genome-wide expression profiles**. *Proc Natl Acad Sci U S A* 2005, **102**(43):15545-15550.
32. Mootha VK, Lindgren CM, Eriksson KF, Subramanian A, Sihag S, Lehar J, Puigserver P, Carlsson E, Ridderstråle M, Laurila E *et al*: **PGC-1alpha-responsive genes involved in oxidative phosphorylation are coordinately downregulated in human diabetes**. *Nat Genet* 2003, **34**(3):267-273.
33. Newman AM, Steen CB, Liu CL, Gentles AJ, Chaudhuri AA, Scherer F, Khodadoust MS, Esfahani MS, Luca BA, Steiner D *et al*: **Determining cell type abundance and expression from bulk tissues with digital cytometry**. *Nat Biotechnol* 2019, **37**(7):773-782.

34. Yoshihara K, Shahmoradgoli M, Martínez E, Vegesna R, Kim H, Torres-Garcia W, Treviño V, Shen H, Laird PW, Levine DA *et al*: **Inferring tumour purity and stromal and immune cell admixture from expression data**. *Nat Commun* 2013, **4**:2612.
35. Li T, Fu J, Zeng Z, Cohen D, Li J, Chen Q, Li B, Liu XS: **TIMER2.0 for analysis of tumor-infiltrating immune cells**. *Nucleic Acids Res* 2020, **48**(W1):W509-w514.
36. Li T, Fan J, Wang B, Traugh N, Chen Q, Liu JS, Li B, Liu XS: **TIMER: A Web Server for Comprehensive Analysis of Tumor-Infiltrating Immune Cells**. *Cancer Res* 2017, **77**(21):e108-e110.
37. Li B, Severson E, Pignon JC, Zhao H, Li T, Novak J, Jiang P, Shen H, Aster JC, Rodig S *et al*: **Comprehensive analyses of tumor immunity: implications for cancer immunotherapy**. *Genome Biol* 2016, **17**(1):174.
38. Uhlen M, Zhang C, Lee S, Sjöstedt E, Fagerberg L, Bidkhori G, Benfeitas R, Arif M, Liu Z, Edfors F *et al*: **A pathology atlas of the human cancer transcriptome**. *Science* 2017, **357**(6352).
39. Thul PJ, Åkesson L, Wiking M, Mahdessian D, Geladaki A, Ait Blal H, Alm T, Asplund A, Björk L, Breckels LM *et al*: **A subcellular map of the human proteome**. *Science* 2017, **356**(6340).
40. Uhlén M, Fagerberg L, Hallström BM, Lindskog C, Oksvold P, Mardinoglu A, Sivertsson Å, Kampf C, Sjöstedt E, Asplund A *et al*: **Proteomics. Tissue-based map of the human proteome**. *Science* 2015, **347**(6220):1260419.
41. Han H, Cho JW, Lee S, Yun A, Kim H, Bae D, Yang S, Kim CY, Lee M, Kim E *et al*: **TRRUST v2: an expanded reference database of human and mouse transcriptional regulatory interactions**. *Nucleic Acids Res* 2018, **46**(D1):D380-d386.
42. Liu CJ, Hu FF, Xia MX, Han L, Zhang Q, Guo AY: **GSCALite: a web server for gene set cancer analysis**. *Bioinformatics* 2018, **34**(21):3771-3772.
43. Siegel RL, Miller KD, Jemal A: **Cancer statistics, 2020**. *CA Cancer J Clin* 2020, **70**(1):7-30.
44. Kamarajah SK, Bundred JR, Marc OS, Jiao LR, Hilal MA, Manas DM, White SA: **A systematic review and network meta-analysis of different surgical approaches for pancreaticoduodenectomy**. *HPB (Oxford)* 2020, **22**(3):329-339.
45. Zhang L, Sanagapalli S, Stoita A: **Challenges in diagnosis of pancreatic cancer**. *World J Gastroenterol* 2018, **24**(19):2047-2060.
46. Wei Q, Mu K, Li T, Zhang Y, Yang Z, Jia X, Zhao W, Huai W, Guo P, Han L: **Deregulation of the NLRP3 inflammasome in hepatic parenchymal cells during liver cancer progression**. *Lab Invest* 2014, **94**(1):52-62.
47. Ma X, Guo P, Qiu Y, Mu K, Zhu L, Zhao W, Li T, Han L: **Loss of AIM2 expression promotes hepatocarcinoma progression through activation of mTOR-S6K1 pathway**. *Oncotarget* 2016, **7**(24):36185-36197.
48. Allen IC, TeKippe EM, Woodford RM, Uronis JM, Holl EK, Rogers AB, Herfarth HH, Jobin C, Ting JP: **The NLRP3 inflammasome functions as a negative regulator of tumorigenesis during colitis-associated cancer**. *J Exp Med* 2010, **207**(5):1045-1056.

49. Williams TM, Leeth RA, Rothschild DE, Coutermarsh-Ott SL, McDaniel DK, Simmons AE, Heid B, Cecere TE, Allen IC: **The NLRP1 inflammasome attenuates colitis and colitis-associated tumorigenesis**. *J Immunol* 2015, **194**(7):3369-3380.
50. Qiu S, Liu J, Xing F: **'Hints' in the killer protein gasdermin D: unveiling the secrets of gasdermins driving cell death**. *Cell Death Differ* 2017, **24**(4):588-596.
51. Saeki N, Usui T, Aoyagi K, Kim DH, Sato M, Mabuchi T, Yanagihara K, Ogawa K, Sakamoto H, Yoshida T *et al*: **Distinctive expression and function of four GSDM family genes (GSDMA-D) in normal and malignant upper gastrointestinal epithelium**. *Genes Chromosomes Cancer* 2009, **48**(3):261-271.
52. Hergueta-Redondo M, Sarrió D, Molina-Crespo Á, Megias D, Mota A, Rojo-Sebastian A, García-Sanz P, Morales S, Abril S, Cano A *et al*: **Gasdermin-B promotes invasion and metastasis in breast cancer cells**. *PLoS One* 2014, **9**(3):e90099.
53. Kamarajah SK, Burns WR, Frankel TL, Cho CS, Nathan H: **Validation of the American Joint Commission on Cancer (AJCC) 8th Edition Staging System for Patients with Pancreatic Adenocarcinoma: A Surveillance, Epidemiology and End Results (SEER) Analysis**. *Ann Surg Oncol* 2017, **24**(7):2023-2030.
54. Parkin DM, Boyd L, Walker LC: **16. The fraction of cancer attributable to lifestyle and environmental factors in the UK in 2010**. *Br J Cancer* 2011, **105 Suppl 2**(Suppl 2):S77-81.
55. Kirkegård J, Mortensen FV, Cronin-Fenton D: **Chronic Pancreatitis and Pancreatic Cancer Risk: A Systematic Review and Meta-analysis**. *Am J Gastroenterol* 2017, **112**(9):1366-1372.
56. Bosetti C, Bertuccio P, Negri E, La Vecchia C, Zeegers MP, Boffetta P: **Pancreatic cancer: overview of descriptive epidemiology**. *Mol Carcinog* 2012, **51**(1):3-13.
57. van Erning FN, Mackay TM, van der Geest LGM, Groot Koerkamp B, van Laarhoven HWM, Bonsing BA, Wilmink JW, van Santvoort HC, de Vos-Geelen J, van Eijck CHJ *et al*: **Association of the location of pancreatic ductal adenocarcinoma (head, body, tail) with tumor stage, treatment, and survival: a population-based analysis**. *Acta Oncol* 2018, **57**(12):1655-1662.
58. Ilic M, Ilic I: **Epidemiology of pancreatic cancer**. *World J Gastroenterol* 2016, **22**(44):9694-9705.
59. Wolpin BM, Bao Y, Qian ZR, Wu C, Kraft P, Ogino S, Stampfer MJ, Sato K, Ma J, Buring JE *et al*: **Hyperglycemia, insulin resistance, impaired pancreatic β-cell function, and risk of pancreatic cancer**. *J Natl Cancer Inst* 2013, **105**(14):1027-1035.
60. Andersen DK, Korc M, Petersen GM, Eibl G, Li D, Rickels MR, Chari ST, Abbruzzese JL: **Diabetes, Pancreatogenic Diabetes, and Pancreatic Cancer**. *Diabetes* 2017, **66**(5):1103-1110.
61. Taabazuing CY, Griswold AR, Bachovchin DA: **The NLRP1 and CARD8 inflammasomes**. *Immunol Rev* 2020, **297**(1):13-25.
62. Fenini G, Karakaya T, Hennig P, Di Filippo M, Beer HD: **The NLRP1 Inflammasome in Human Skin and Beyond**. *Int J Mol Sci* 2020, **21**(13).
63. Ratushny V, Gober MD, Hick R, Ridky TW, Seykora JT: **From keratinocyte to cancer: the pathogenesis and modeling of cutaneous squamous cell carcinoma**. *J Clin Invest* 2012, **122**(2):464-472.

64. Voiculescu VM, Lisievici CV, Lupu M, Vajaitu C, Draghici CC, Popa AV, Solomon I, Sebe TI, Constantin MM, Caruntu C: **Mediators of Inflammation in Topical Therapy of Skin Cancers**. *Mediators Inflamm* 2019, **2019**:8369690.
65. Shibamoto M, Hirata H, Eguchi H, Sawada G, Sakai N, Kajiyama Y, Mimori K: **The loss of CASP4 expression is associated with poor prognosis in esophageal squamous cell carcinoma**. *Oncol Lett* 2017, **13**(3):1761-1766.
66. Wang Z, Ni F, Yu F, Cui Z, Zhu X, Chen J: **Prognostic significance of mRNA expression of CASPs in gastric cancer**. *Oncol Lett* 2019, **18**(5):4535-4554.
67. Papoff G, Presutti D, Lalli C, Bolasco G, Santini S, Manelfi C, Fustaino V, Alemà S, Ruberti G: **CASP4 gene silencing in epithelial cancer cells leads to impairment of cell migration, cell-matrix adhesion and tissue invasion**. *Sci Rep* 2018, **8**(1):17705.
68. Terlizzi M, Colarusso C, De Rosa I, De Rosa N, Somma P, Curcio C, Sanduzzi A, Micheli P, Molino A, Saccomanno A *et al*: **Circulating and tumor-associated caspase-4: a novel diagnostic and prognostic biomarker for non-small cell lung cancer**. *Oncotarget* 2018, **9**(27):19356-19367.
69. Meng L, Tian Z, Long X, Diao T, Hu M, Wang M, Zhang W, Zhang Y, Wang J, He Y: **Caspase 4 Overexpression as a Prognostic Marker in Clear Cell Renal Cell Carcinoma: A Study Based on the Cancer Genome Atlas Data Mining**. *Front Genet* 2020, **11**:600248.
70. Terlizzi M, Colarusso C, De Rosa I, Somma P, Curcio C, Aquino RP, Panico L, Salvi R, Zito Marino F, Botti G *et al*: **Identification of a novel subpopulation of Caspase-4 positive non-small cell lung Cancer patients**. *J Exp Clin Cancer Res* 2020, **39**(1):242.
71. Terlizzi M, Molino A, Colarusso C, Somma P, De Rosa I, Troisi J, Scala G, Salvi R, Pinto A, Sorrentino R: **Altered lung tissue lipidomic profile in caspase-4 positive non-small cell lung cancer (NSCLC) patients**. *Oncotarget* 2020, **11**(38):3515-3525.
72. Dey P, Kimmelman AC, DePinho RA: **Metabolic Codependencies in the Tumor Microenvironment**. *Cancer Discov* 2021, **11**(5):1067-1081.
73. Kim MP, Li X, Deng J, Zhang Y, Dai B, Allton KL, Hughes TG, Siangco C, Augustine JJ, Kang Y *et al*: **Oncogenic KRAS Recruits an Expansive Transcriptional Network through Mutant p53 to Drive Pancreatic Cancer Metastasis**. *Cancer Discov* 2021, **11**(8):2094-2111.
74. Najafi M, Hashemi Goradel N, Farhood B, Salehi E, Nashtaei MS, Khanlarkhani N, Khezri Z, Majidpoor J, Abouzaripour M, Habibi M *et al*: **Macrophage polarity in cancer: A review**. *J Cell Biochem* 2019, **120**(3):2756-2765.
75. Cao Y, Dong L, He Y, Hu X, Hou Y, Dong Y, Yang Q, Bi Y, Liu G: **The direct and indirect regulation of follicular T helper cell differentiation in inflammation and cancer**. *J Cell Physiol* 2021, **236**(8):5466-5480.
76. Wu M, Li X, Liu R, Yuan H, Liu W, Liu Z: **Development and validation of a metastasis-related Gene Signature for predicting the Overall Survival in patients with Pancreatic Ductal Adenocarcinoma**. *J Cancer* 2020, **11**(21):6299-6318.

Figures

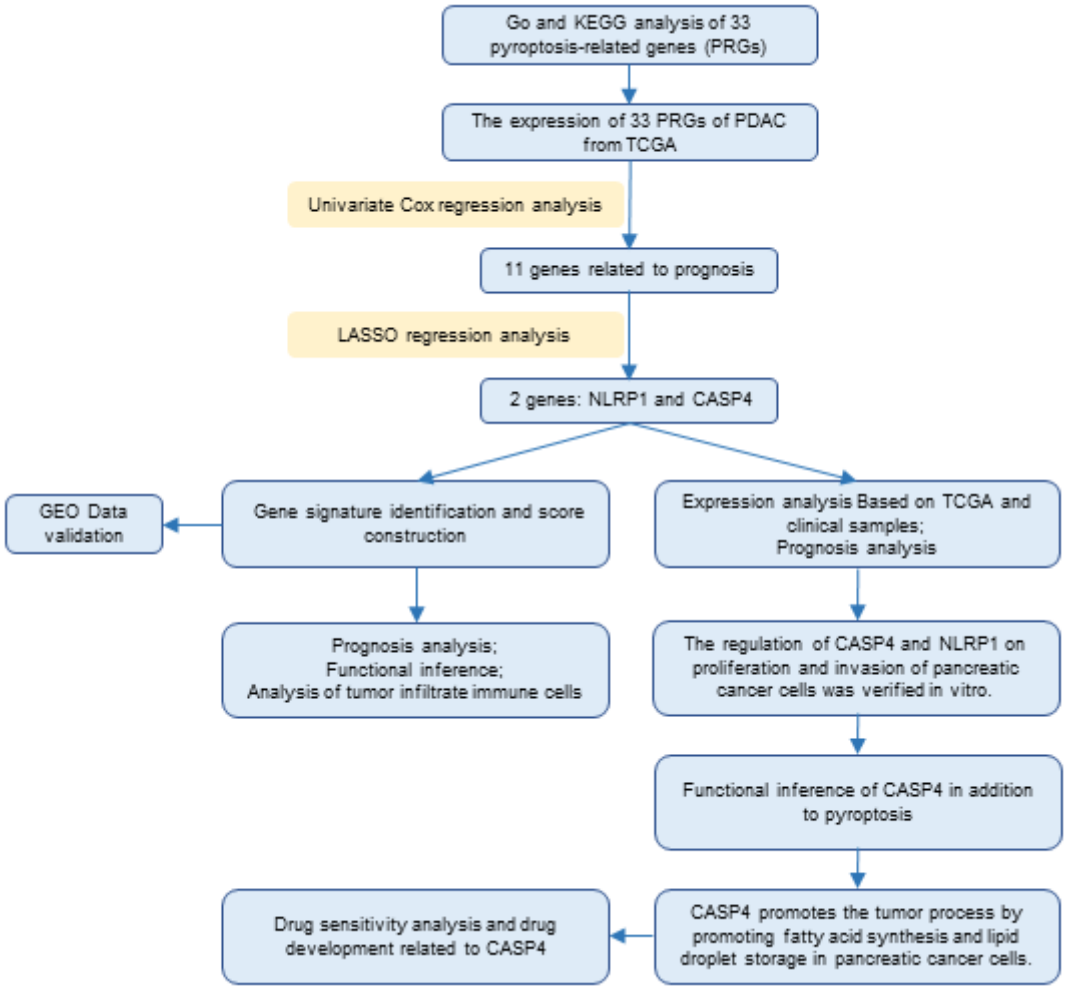

Figure 1

The flow chart of the present study.

Figure 2

GO and KEGG pathway enrichment analysis of 319 glycolysis-related genes selected from GSEA. (A) The bar plot of GO pathway enrichment analysis. (B) The bar plot of KEGG pathway enrichment analysis. (BP: biological process; CC: cell component; MF: molecular function)

Figure 3

Identification of a 2-PRGs signature for PDAC patients and detection of predictive performance (A) LASSO Cox regression was used to select the most powerful parameter with cross-validation. (B) Kaplan-Meier survival analysis of PDAC patients in different risk groups from TCGA-PAAD cohort (C-D) The distribution of risk score and survival status. (E) The ROC based on risk score. (The risk score was divided into high-risk group and low-risk group with a cut-off value of 50%.) (F) Tree diagram of a univariate regression analysis. (G) Tree diagram of a multivariate regression analysis. (** P < 0.01, *** P < 0.001.) (note: Patients with tumors located in the body and tail of the pancreas received distal pancreatectomy, and patients with tumors located in the head of the pancreas received Whipple surgery.)

Figure 4

External validation of the risk prediction model using GSE57495 dataset. (A) Kaplan-Meier survival analysis of PDAC patients in the high-risk group and low-risk group. (B) The ROC based on risk score. (C-D) The distribution of risk score and survival status.

Figure 5

External validation of the risk prediction model using GSE62452 dataset. (A) Kaplan-Meier survival analysis of PDAC patients in the high-risk group and low-risk group. (B) The ROC based on risk score. (C-D) The distribution of risk score and survival status.

Figure 6

Expression and survival analysis of PEGs in PDAC. (A) The differential expression of CASP4 in PDAC and para-cancer tissues. The box plot showed the statistical significance of differential expression assessed by Wilcoxon test (* p < 0.05). (B) Methylation levels of CASP4 at chr11:104838825-104841325 and chr11:104826922-104829422 in PDAC and para-cancer tissues. (C) The correlation plot of NLRP1 and CASP4 by Pearson test. (D&E) The Kaplan-Meier OS survival curves of NLRP1 and CASP4 mRNA expression level in PDAC. (F&G) The Kaplan-Meier OS survival curves of NLRP1 and CASP4 protein expression level in PDAC. (H) The protein expression score of staining and intensity of NLRP1 and CASP4 proteins in all PDAC samples. Protein expression score is based on immunohistochemical data manually

scored with regard to staining intensity (negative, weak, moderate or strong) and fraction of stained cells (<25%, 25-75% or >75%). (I&J) Immunohistochemical staining of NLRP1 and CASP4 proteins in PDAC.

Figure 7

PRGs regulate the proliferation and invasion of pancreatic cancer cells in vitro (A-B) After siRNA transfection, qPCR and western blot was used to detect RNA and protein expression levels of CASP4 and NLRP1 respectively in PANC-1 cells. (C) CCK8 assay was used to detect the proliferation of PANC-1 cells after transfection with siRNA. (D) Transwell was used to detect the change of cell invasion ability after transfection with siRNA. (**P<0.01, ***P<0.001)

Figure 8

CASP4 was associated with KRAS and P53 mutations potentially

(A&B) Cloud plot and waterfall plot of mutant landscape in TCGA-PAAD samples. (C) The expression levels of CASP4 were different in KRAS mutation, P53 mutation and wild-type tumor tissues respectively. (D) Correlation curve between CASP4, KRAS and P53 expression levels based on TCGA database. (E) GSEA analysis of differential genes in high CASP4 expression group. (***P<0.001)

Figure 9

CASP4 promoted tumor progression by regulating accumulation of lipid droplets

(A) RNA expression level of key enzyme molecules in fatty acid synthesis after transfecting shCASP4 in PANC-1 cells. (B) The mean number of lipid vesicles per cell. The lipid droplets were counted randomly (≥50 cells were counted per condition). (*P<0.05, ***P<0.001)

Figure 10

Analysis of drug sensitivity associated with PEGs. Red is positive correlation, which means the higher the gene expression, the more sensitive to the drug, while the blue is the opposite.

Supplementary Files

This is a list of supplementary files associated with this preprint. Click to download.

- Supplementarymaterial.docx